

Group velocity estimation of Lamb waves based on the wavelet transform

D. Waltisberg¹, R. Raišutis²

¹ Department of Information Technology and Electrical Engineering, Swiss Federal Institute of Technology, Zurich, Switzerland, E-mail: wdaniel@ee.ethz.ch

² Ultrasound Institute of Kaunas University of Technology, Kaunas, Lithuania, E-mail: renaldas.raisutis@ktu.lt

Abstract

Lamb waves are often used in ultrasonic applications for non-destructive testing of large constructions. The difficulty in the analysis of Lamb waves is their dispersive characteristics, especially their frequency dependent phase and group velocities. This article focuses on the separation of the first symmetric mode S_0 and the first asymmetric mode A_0 and the reliable estimation of their group velocities. Starting from the analysis of the received ultrasonic signals at different distances from the source, three methods were implemented to estimate the group velocity. The best results were obtained by performing the wavelet transform on these signals and using the similarity of the coefficient lines for different distances between the transmitter and the receiver. The group velocity estimation was used to visualise the segment of the dispersion curve of a narrowband signal. The wavelet transform allowed taking a closer look to the particular mode of guided waves in the time and frequency space.

Keywords: wavelet transform, Lamb wave, guided wave, group velocity.

1. Introduction

The usage of guided waves in a non-destructive testing of large structures is promising, because Lamb waves are propagating along the surface over long distances and allow examination of large surfaces at once [1]. The difficulty with guided waves is their complicated features, depending on a frequency, thickness of the plate and material properties [2]. Moreover, the excitation of multiple modes is inevitable. These properties make the interpretation of the received signals complicated and imply the need of a signal processing.

The wavelet transform performs a time-frequency analysis of the ultrasonic signal, with a sufficient resolution in the frequency and time domains for practical applications. Analysis of the effects of the dispersive characteristics to the continuous wavelet transform were carried out using the wavelet propagator proposed by Kulesh et al. [3]. Based on these results, three methods for estimation of the group velocity values for particular modes of guided waves were implemented by us and compared.

2. Wavelet transform

The main concept of the wavelet transform is the decomposition of the signal $s(t)$ into a sum of so called *daughter* wavelets $\psi_{a,b}(t)$. These wavelets are shifted and translated versions of the *mother* wavelet $\psi(t)$ [4]:

$$\psi_{a,b}(t) = \frac{1}{\sqrt{|a|}} \psi\left(\frac{t-b}{a}\right), \quad (1)$$

where t is the time, b is the delay, a is the scale parameter.

There exist many different families of mother wavelets. They differ in properties like orthogonality, symmetry or vanishing moments.

The continuous wavelet transform (CWT) of the signal $s(t)$ related to the daughter wavelet $\psi_{a,b}(t)$ is given by

$$\begin{aligned} CWT_s^\psi(b, a) &= \int_{-\infty}^{+\infty} s(t) \cdot \psi_{a,b}^*(t) dt = \\ &= \frac{1}{\sqrt{|a|}} \int_{-\infty}^{+\infty} s(t) \cdot \psi^*\left(\frac{t-b}{a}\right) dt \end{aligned}, \quad (2)$$

where $*$ denotes the complex conjugation [4]. This decomposition is redundant and for some applications, the scale parameter a and the translation parameter b are performed in a special manner to get the discrete wavelet transform (DWT). In our investigation, we will stay with the continuous wavelet transform. The reason is that we want to get as much information from the wavelet transform as possible, even if the information is redundant.

The relation between the Fourier transform

$$\hat{s}(f) = \int_{-\infty}^{+\infty} s(t) e^{-2i\pi \cdot f \cdot t} dt, \quad (3)$$

and the CWT (Eq. 2) is given by

$$CWT_s^\psi(b, a) = \sqrt{|a|} \cdot \int_{-\infty}^{+\infty} \hat{\psi}^*(af) \cdot \hat{s}(f) \cdot e^{2\pi \cdot i \cdot f \cdot b} df. \quad (4)$$

In dispersive and dissipative materials, the relation between two signals $s_1(t)$ and $s_2(t)$ separated at distance d can be represented by the Fourier transform [3]. With the wave number $k(f)$ and the attenuation function $\alpha(f)$, the relation is then given by

$$\hat{s}_2(f) = e^{-i \cdot 2 \cdot \pi \cdot d \cdot k(f)} \cdot e^{-d \cdot \alpha(f)} \cdot \hat{s}_1(f); \quad (5)$$

This corresponds to the continuous wavelet transform of

$$\begin{aligned} CWT_{s_2}^\psi(b, a) &= \sqrt{|a|} \cdot \int_{-\infty}^{+\infty} \hat{s}_1(f) \cdot \hat{\psi}^*(af) \cdot e^{-i \cdot 2 \cdot \pi \cdot d \cdot k(f)} \times \\ &\quad \times e^{2\pi \cdot i \cdot f \cdot b} e^{-d \cdot \alpha(f)} df. \end{aligned} \quad (6)$$

With the assumption that the attenuation function $\alpha(f)$ and the wavenumber $k(f)$ are varying slowly with respect to the effective size of the spectrum of the wavelet transform, we can use the approximation proposed by Kulesh et al. [3] and approximate $\alpha(f)$ and $k(f)$ by the first terms of its Taylor series around the central frequency f_c :

$$\alpha(f) = \alpha(f_c) + O(|f - f_c|), \quad (7)$$

$$k(f) = k(f_c) + (f - f_c) \cdot k'(f_c) + O(|f - f_c|^2), \quad (8)$$

where $k'(f_c)$ denotes the derivation of k with respect to f at the frequency f_c and $O(x^y)$ denotes the ‘big O notation’, which indicates that the error term is smaller than x^y for x close to zero.

These approximations lead to

$$CWT_{s_2}^\psi(b, a) = e^{-d \cdot \alpha(f_c)} \cdot e^{-2 \cdot \pi \cdot i \cdot d [k(f_c) - f_c \cdot k'(f_c)]} \times CWT_{s_1}^\psi(b - d \cdot k'(f_c), a), \quad (9)$$

This equation shows that the absolute parts of the CWT of the two signals differ only in the shift of $\sigma = d \cdot k'(f_c)$ and the attenuation factor [5]. This can be justified by another assumption. The pseudo frequency of a daughter wavelet f_p can be linked to the fixed scale parameter a . The dispersive characteristic of the wave implies that the velocity is frequency dependent, but for a fixed pseudo frequency there exists only one velocity. Therefore, the shape of the coefficients should be equal for different distances from the origin.

The group velocity v_{group} is related reciprocally to the derivation of the wave number $k'(f_c)$ and leads to

$$v_{group} = \frac{1}{k'(f_c)} = \frac{d}{\sigma}. \quad (10)$$

3. Experimental set-up

The stainless thin steel plate (thickness 1mm) was investigated by wedge type (45°) ultrasonic transducers of

the central frequency 500 kHz. The contact type measurement set-up was applied, oil was used as a coupling liquid. The measurements were performed with the scanning step of 10 mm of the receiver away from the transmitter and the sampling frequency of 50 MHz. Twelve measurements were executed at different positions the receiver. The resulted B-scan with the indicated modes of the guided waves is presented in Fig.1. The ultrasonic signals obtained at the measurement step 1 and at the measurement step 12 are presented in Fig.2.

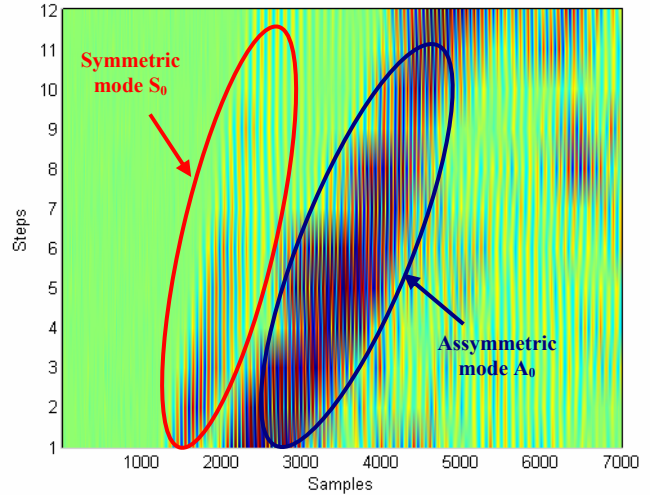


Fig.1. Measured B-scan image, two modes of guided waves with different group velocities can be identified: symmetric S_0 mode, asymmetric A_0 mode

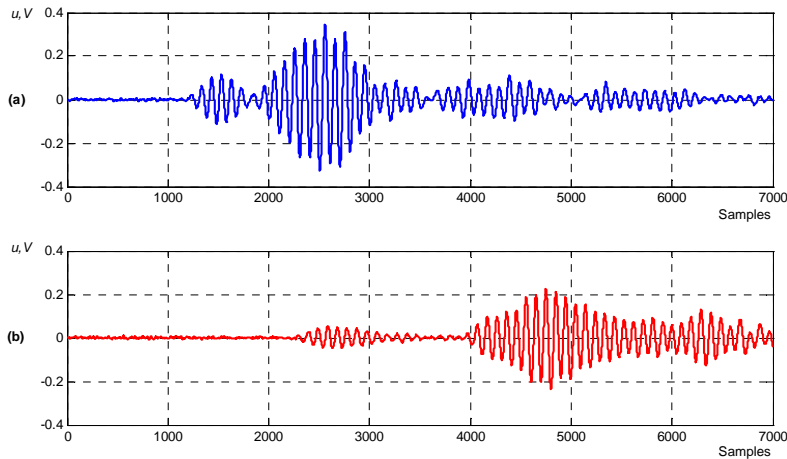


Fig.2. Ultrasonic signals received at measurement points at 10mm (a) and 120mm (b) away from the transmitting transducer.

4. Methods for group velocity estimation

The task is to find the group velocity considering the twelve measured ultrasonic signals at different positions from the receiver. Three different methods were implemented, see Fig.3. For each guided wave mode whose group velocity has to be estimated, these steps have to be executed.

The first step is to choose a window of the signals in the time domain. If possible, there should be no interference with other waves in this window.

In the first method, called ‘Maximal Value’, the points with the maximal amplitude values of the ultrasonic signals are computed. It is assumed that these maxima correspond to the same points of the propagating wavefront. The group velocity with the least squared error

is computed. This method does not need any wavelet transform and is mainly used for comparison reason.

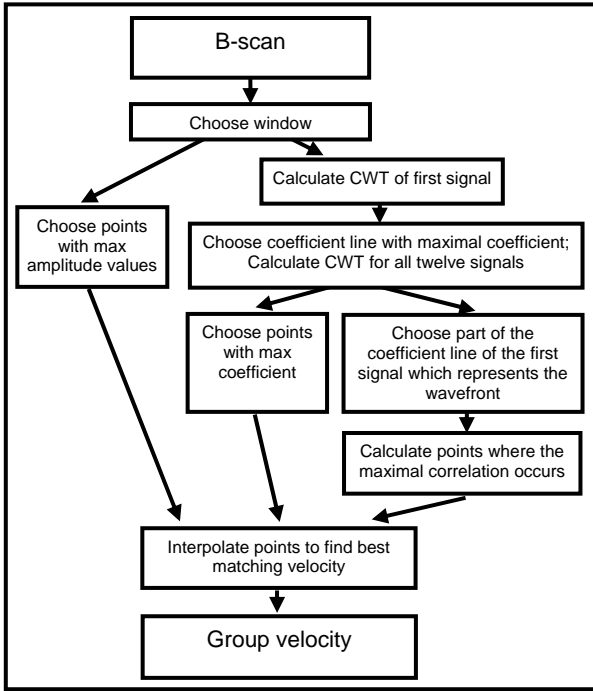


Fig.3. Three different methods for the computation of the group velocity from experimentally measured signals

For the two other methods, the CWT for the signal obtained at 10mm away from the receiver was computed, $CWT_{s_1}^{\psi}(b,a)$. The mother wavelet was decided to be the real Gaussian wavelet of level 8. The scale a_{max} in which the coefficient with maximal value occurs was calculated and for each of the twelve signals, the CWT for the fixed scale a_{max} was computed, $CWT_{s_1}^{\psi}(b,a_{max}), \dots,$

$$CWT_{s_{12}}^{\psi}(b,a_{max}).$$

The second method, called 'Maximal Coeff', computes now the position of the maximal wavelet coefficients for each measured signal. Knowing these points allows the computation of the group velocity for the particular mode. This calculation was carried out using Eq. 10 of the previous section.

In the third method, called 'Maximal Corr', a window that represents the coefficients of the wavefront is chosen. This window is correlated with the other ultrasonic signals obtained at the different distances away from the transmitter in order to find the best matching position for each signal. From these calculated positions, the group velocity can be computed.

4.1 Results of the analysis of the S_0 mode

After the analysis using the previously presented algorithm (Fig. 3), the all methods showed the estimated averaged value of the group velocity close to 5.26 km/s at the central frequency of the transducers.

Although, it seems that the S_0 mode wave of the first signal is separated from the A_0 mode wave, see Fig.2 a, the CWT was influenced by the slow wave (A_0 mode) and the

initially implementation of the method 'Maximal Corr' couldn't show reliable results. After using the fourth signal as a reference signal, the correlation showed good results. The coefficient line with the highest value was calculated to be $a_{max}=64$ corresponding to the pseudo frequency $f_p=468.8$ kHz. In Fig.4, the part of the coefficient line of the signals 1, 4 and 12 representing the fast wave (S_0 mode) is presented, properly aligned by the computed group velocity. The influence of the A_0 mode wave to the coefficients in the first signal can be seen.

Fig 5 shows the shifted waveform of the S_0 mode wave of the signals at measurement steps 1, 4, 8 and 12 away from the transmitter, aligned with the computed group velocity. Although there are some changes in the shape of the waveform, the waveforms match with sufficient a accuracy for practical applications. This shows that the group velocity was estimated correctly enough.

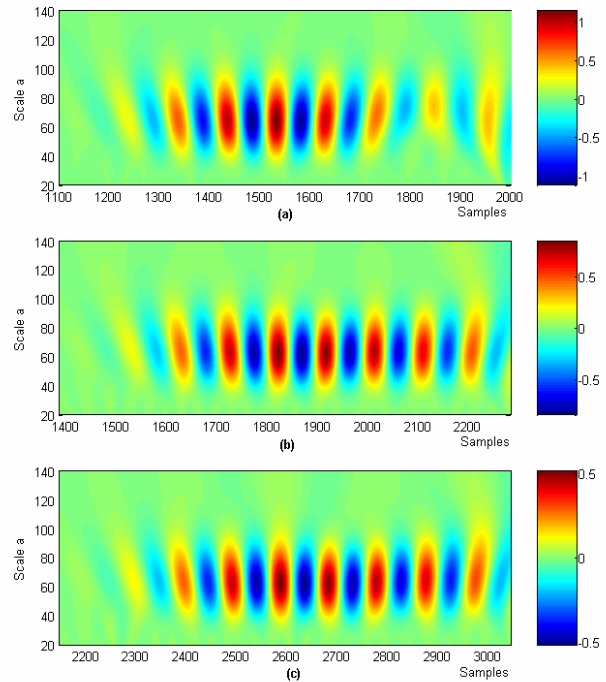


Fig.4. The coefficient lines of the symmetric mode S_0 for the first (a), fourth (b) and twelfth (c) measured signal.

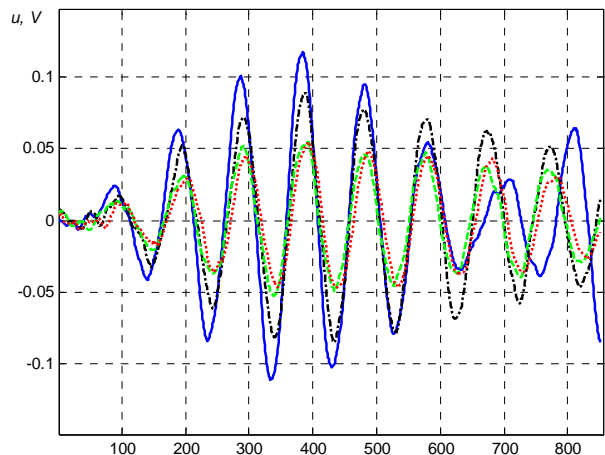


Fig.5. The S_0 wave shifted according to the computed group velocity (blue solid line - measurement step 1, black dash dotted line - measurement step 4, green dashed line - measurement step 8, red dotted line - measurement step 12)

4.2 Results of the analysis of the A_0 mode wave

The estimation of the group velocity for the A_0 mode had to be performed in a more advanced way. The coefficient line with the highest value was calculated to be $a_{max}=66$. In Fig.6, the part of the coefficient line of the signals 1, 4 and 12 representing the slow wave (A_0 mode) is presented, properly aligned by the computed group velocity.

For the methods 'Maximal Value' and 'Maximal Corr', the points that were part of the same wavefront were calculated, see '+' signs at Fig.7. The interpolation of these points to find the group velocity with a least squared error showed different results for each particular method. See Table 1 for the resulting averaged velocities and relative errors.

Table 1: Calculated group velocities using different methods for A_0 mode

	Max Value	Max CWT Coeff	Max Correlation
Velocity (km/s)	2.41	2.40	2.39
Relative error	0.069 %	0.102 %	0.039 %

In Fig.8 the coefficient line and the signal for several measurement steps are plotted. The more regular shape of the coefficient line is a clear advantage and justifies the use of the correlation function in the wavelet domain.

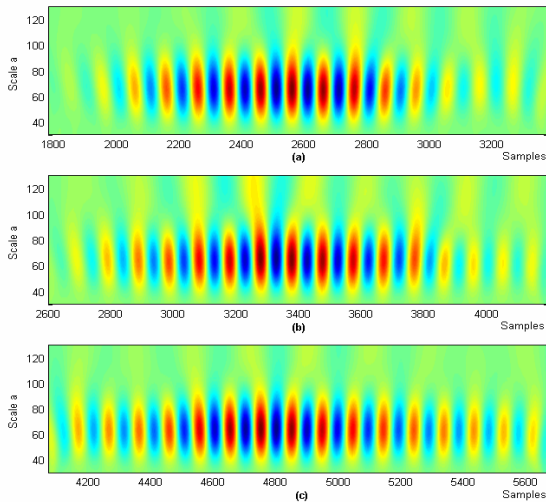


Fig.6. The coefficient lines of the A_0 mode wave for the first (a), fourth (b) and twelfth measured signal (c).

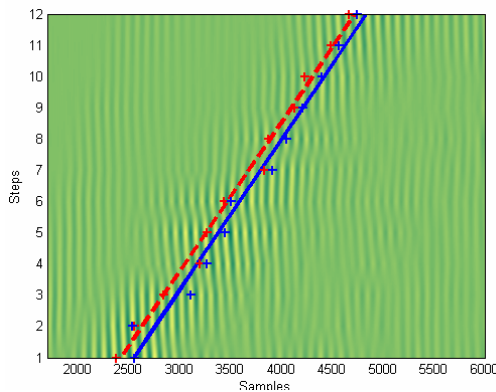


Fig.7. Calculated points belonging to the same positions of the A_0 mode wavefront and their corresponding best matching line (blue solid line - 'Maximal Value', red dashed line - 'Maximal Corr')

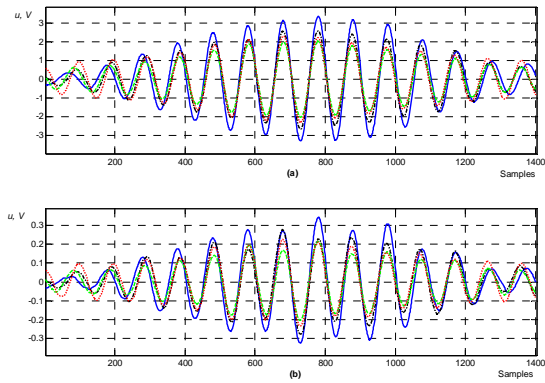


Fig.8. The A_0 mode wave moved by the point with the max correlation: (a) coefficient line for $a=66$, (b) real signal (blue solid line - measurement step 1, black dash dotted line - measurement step 4, green dashed line - measurement step 8, red dotted line - measurement step 12)

4.3 Reconstruction of the dispersion curves segments

The next step in the investigation was the extraction of a segment of the group velocity dispersion curve from the measured B-scan data for particular modes: symmetric S_0 and asymmetric A_0 . The theoretical dispersion curves for the stainless steel plate of thickness 1 mm, density 7890 kg/m^3 , longitudinal velocity 5790 m/s and shear velocity 3100 m/s computed by the global matrix numeric model [8] are presented in Fig.9 a.

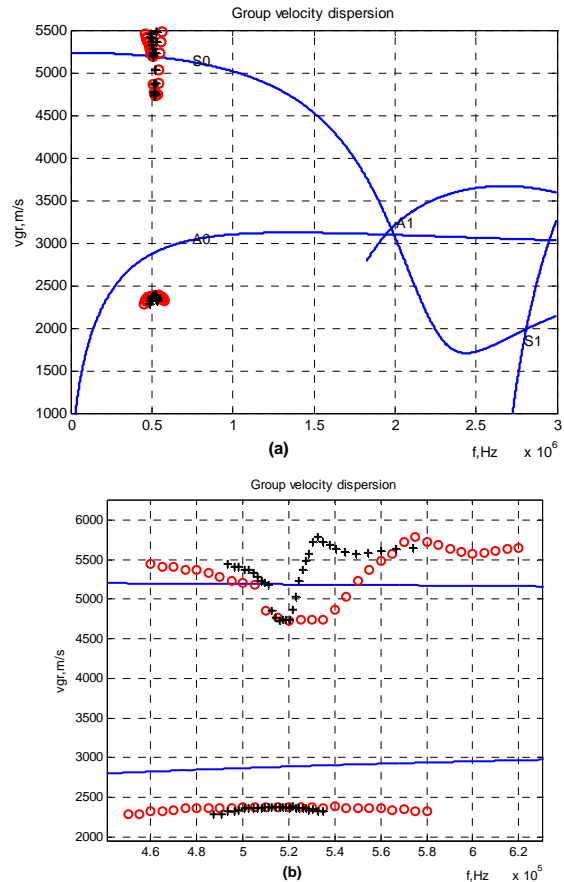


Fig.9. The dispersion curves for the stainless steel plate of thickness 1 mm (a) and zoomed segment of dispersion curves in the vicinity of the frequency bandwidth of the used ultrasonic transducer (b), the separate points indicates experimentally estimated values.

The points of the dispersion curve segment were obtained by filtering the each signal from B-scan with a narrowband filter of incremental changing central frequency $f_{c,i}$ and using a modified version of the 'Maximal Corr' method in order to find the group velocity value corresponding to the central frequency of the filter.

The signals received by the ultrasonic receiver showed a very narrowband characteristic leading to the band of interest from $f_L=450$ kHz up to $f_H=580$ kHz. For the filtering, we used have narrow bandpass filters having a Gaussian envelope, proposed by [9]:

$$S_i(f) = \frac{1}{\sqrt{\pi}} \cdot e^{-\left(\frac{f-f_{c,i}}{B}\right)^2} \quad (11)$$

The central frequencies of the filters were chosen to be in the described band of interest and were increase by $\Delta f=50$ kHz for each filtering step, which leads to the central frequencies $f_{c,i}=f_L+i \Delta f$, $i=1, \dots, 26$. The parameter of the narrowband filter B was chosen to be 5 kHz.

To obtain the filtered B-scan image, the filters were used with each signal $u_k(t)$ (from B-scan) obtained at the measurement step k in order to get the filtered signal $u_{k,i}(t)$:

$$u_{k,i}(t) = IFT[FT(u_k(t)) \cdot S_i(f)], \quad i=1, \dots, 26. \quad (12)$$

The power spectral density (PSD) of the filtered signal was estimated using the Welch's method and the frequency value corresponding to the maximal value of magnitude had been matched to each measured signal. It had been recognised, that there was a difference between the estimated frequency using the Welch's method and the central frequency of the used filter.

The estimation of the group velocity of each filtered B-scan image was performed using a modified version of the 'Maximal Corr' method. At first, the complex Gaussian wavelet was assumed to be the mother wavelet and the coefficients that were compared by us were the absolute values of the coefficients of the complex wavelet transform. The plot of the absolute values of the coefficients of the continuous wavelet transform of the B-scan image filtered by the bandpass filter of $f_{c,i}=520$ kHz for the fixed scale $a=85$ is presented in Fig.10. The estimated maximal frequency using the Welch's method was 516 kHz. The calculated points belonging to the same positions of the A_0 (blue dashed line) and S_0 (red solid line) mode wavefront and their corresponding best matching line are included.

To have as small interference with wavefronts of other modes and reverberations as possible, the coefficients received at ninth measurement step were used as a reference and the analysis window was chosen to be around the maximal values of the absolute values of the CWT.

The choice of the scale of the coefficient line a_{max} was carried out for each filtered B-scan image by calculating the scale at which the maximal coefficients of the wavelet transform occurred.

The result of the group velocity estimation for each filtered B-scan is presented in Fig.9. The frequencies of the red 'o' are the central frequencies of the used filters and the frequencies of the green '+' correspond to the frequencies calculated using the Welch's method. The

group velocities were computed using the modified 'Maximal Corr' method. Fig. 9 b shows the theoretical and measured segment of the dispersion curve over the frequency band of the used ultrasonic transducer.

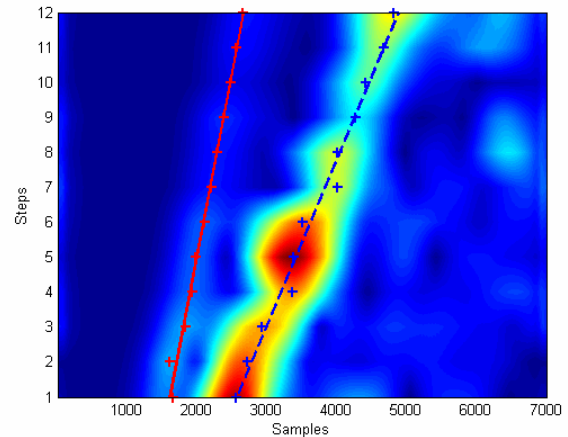


Fig.10. Plot of the absolute coefficients of the CWT of the B-scan image filtered by the bandpass filter of $f_{c,i}= 520$ kHz for the fixed scale $a=85$.

Conclusion

During the examination of the particular modes of the guided waves and their group velocities, the three methods were compared. The 'Maximal Value' method showed good results, but is limited to the maximal amplitude of the signals and does not include any parameters that allow adjusting. Errors occurred when the particular mode had several maxima or due to measurements uncertainties (for example, (loss of the acoustic contact between the transducer and the plate, or overlapped signals).

The 'Maximal Coeff' method couldn't show better results than the previous one. The main reason is due to the fact that higher amplitude values of the signal in the time domain lead also to higher coefficient values in the time-frequency domain.

The 'Maximal Corr' method showed enough good results. Due to the similarity of the coefficients in the wavelet domain and the smoothing through the wavelet transform, the position of the same mode of the guided waves was determined with a high accuracy. This method gives also the possibility to adjust some parameters, like choice of the samples used for the selected analysis window, in order to get the best results.

It can be concluded that the advantages of the wavelet transform are on one hand the smoothing of the coefficients and the similarity in the shape of the coefficients that give a good performance of the use with the correlation. On the an other hand, the calculation of wavelet transform at different measurement points gives an opportunity of a deeper insight into the frequency and time dependence of the signal's features which can be used to verify the values of the calculated group velocities.

The estimated values of the group velocity from the measured signals were compared with theoretical calculations. The obtained results show that it is possible reliably to reconstruct the segment of the dispersion curve from the experimental results using the narrowband filtering technique. The obtained results are reliable inside the bandwidth of the used ultrasonic transducer.

References

1. **Cawley P., Lowe M. J. S., Alleyne D. N, Pavlakovic B. and Wilcox P.** Practical long range guided wave testing: Applications to Pipes and Rail, Mat. Evaluation. 2003. Vol. 61. P.66-74.
2. **Rose J. L.** Ultrasonic waves in solid media. Cambridge University Press 1999.
3. **Kulesh M., Holschneider M., Diallo M. S., Xie Q. and Scherbaum F.** Modeling of wave dispersion using continuous wavelet transforms. Pure and Applied Geophysics. 2005. Vol. 162. P.843–855.
4. **Daubechies I.** Ten Lectures on Wavelets. SIAM. 1992.
5. **Holschneider M., Diallo M. S., Kulesh M., Ohrnberger M., Lück E. and Scherbaum F.** Characterization of dispersive surface waves using continuous wavelet transforms. Geophys. Journal. International. 2005. Vol. 163. P.463–478.
6. **Butėnas G. and Kažys R.** Application of time reversal approach for focusing of Lamb waves. Ultragarsas. 2007. Vol.62. No.2. P.38-43.
7. **He P.** Simulation of ultrasound pulse propagation in lossy media obeying a frequency power law. IEEE Trans. Ultrason., Ferroelect., Freq. Contr. January 1998. Vol.45. No.1. P.114-125.
8. **Demčenko, L. Mažeika:** Calculation of Lamb waves dispersion curves in multi-layered planar structures. Ultragarsas. 2002. No.44. P.15–17.
9. **Raišutis R., Voleišis A., Kažys R.** Application of the through transmission ultrasonic technique for estimation of the phase velocity dispersion in plastic materials. Ultragarsas. 2008. Vol.63. No.3. P. 15-18.

D. Waltisberg, R. Raišutis

Lembo bangų grupinio greičio verčių nustatymas naudojant bangelių transformaciją

Reziumė

Lembo bangos plačiai naudojamos ultragarsiniuose didelių gabaritų konstrukcijų tyrimuose. Šiomis bangomis gautų rezultatų interpretavimą komplikuoja šių bangų dispersinės charakteristikos, tai yra nuo dažnio priklausantys faziniai ir grupiniai greičiai. Šis darbas skirtas simetrinei ir asimetrinei modoms išskirti ir jų grupinio greičio vertėms nustatyti. Grupinio greičio vertės buvo nustatomos trimis būdais. Geriausių rezultatų gauta atlikus ultragarsinių signalų bangelių transformaciją ir panaudojus koeficientų panašumo vertes, gautas skirtingiems atstumams tarp siuntiklio ir ėmiklio. Bangelių transformacija leidžia detaliau nagrinėti konkrečią pasirinktą modą laiko-dažnio srityje.

Patekta spaudai 2008 12 15